JOURNAL OF OPTOELECTRONICS AND ADVANCED MATERIALS Vol. 14, No. 11- 12, November – December 2012, p. 910 - 917

Role of thickness in physical properties of Cu_2S thin films prepared by vacuum evaporation method

M. RAMYA*, S .GANESAN[a]
Department of Physics, Sri Shakthi Institute of Engg. & Tech., Coimbatore 641 062, Tamil Nadu, India
[a]*Department of Physics, Government College of Technology., Coimbatore 641 062 ,Tamil Nadu, India*

Transparent semi-conducting copper sulphide thin films with good crystallinity have been deposited on glass substrates by vacuum evaporation method. The synthesized Cu_2S thin films were characterized using various techniques without any annealing treatment. Structural, optical and electrical properties of the films have been studied for different film thicknesses. Films prepared at relatively higher thickness is found to be high conductive in nature. Hall effect measurements were carried out to determine the electrical properties of the film. Hall measurements of the films showed p-type conduction nature with a carrier concentration in the range 10^{19}–10^{22} cm^{-3}. It is found that the deposited lower thickness Cu_2S films have particle size of the order of 207 nm. Optical measurements of the film were carried out to calculate band gap energy of the material. Current voltage characteristics of different film thicknesses have been studied and it is observed that in the low voltage region, the conduction current obeys Ohm's law. Photosensitivity of the material enhances with light intensity.

(Received May 31, 2012; accepted October 30, 2012)

Keywords: Copper sulphide, grain size, P-type conduction, Hall -effect measurement

1. Introduction

Copper sulphides were largely investigated in recent years due to its interesting optical and electrical properties that result from the variations in stoichiometry, composition and morphology. Copper sulfide (Cu_xS) usually exhibits semi-metallic properties, intrinsic semi-conductivities and in some cases, ductility. Cu_xS forms p-type transparent film in the bulk form [1] and exists in five stable phases where x falls in the range between 1 and 2. Copper content variation impacts on both electrical conductivity and optical band gap properties and hence makes these compounds potentially useful in wide range of applications. While the copper sulfides have not been extensively characterized by Raman spectroscopy, they have been characterized electrochemically. Free energies and reduction potentials, obtained by constant current experiments on thin film electrodes, have been determined for chalcocite [Cu_2S], djurleite [$Cu_{1.95-1.91}S$], digenite [$Cu_{1.86-1.80S}$], anilite [$Cu_{1.75-1.65}S$] and covellite [CuS] as well as the blue remaining co-vellite [$Cu_{1.40-1.12}S$] (spionkopite and yarrowite)[2]. It is well known that Cu_xS has distinct compositions because of the variation in x, $1< x <2$ with different stoichiometry and that oxidation and temperature is responsible for change from one composition to another. It is interesting to note that these distinct compositions are not remarkable for the change in crystallite structure but in the variation of electrical resistivity and optical band gap energy [3,4]. Since stoichiometric difference between various phases of Cu_xS is small, it becomes highly challenging task in obtaining a controlled stoichiometry of Cu_2S thin films. Among various metal chalcogenide semiconductor materials, copper sulphide thin films have been identified as a potential material for future applications in optoelectronic device like fluorescent devices [5]. The most striking benefit obtained by utilizing Cu_2S as sensor material is the low operating temperature for sensor applications [6]. It has been experimentally established that preparation method and conditions strongly influence the structural properties of the films. Among the widely used method such as CBD, CVD, Cu_2S thin film can also be deposited using solvo thermal method, solid state reaction [7], vacuum evaporation [8] and microwave technique. In the present work Cu_2S thin films were deposited by vacuum evaporation method and the goal of the work was therefore to study the physical properties of the film such as carrier concentration, carrier mobility, resistivity and dielectric properties of Cu_2S thin films as a function film thickness.

2. Experimental details

High purity (99.99%) copper sulphide powder was utilized for evaporation. Cu_2S of different thicknesses were deposited onto properly cleaned flat glass substrates with the help of a Hind High Vacuum Coating unit (HINDHIVAC 12A4) under the pressure of 10^{-6} Pa. The glass substrates are rinsed with distilled water and placed in an ultrasonic cleaner where they are agitated for 30 minutes by soap solution and then cleaned with iso-propyl alcohol. Next the glass substrates are heated in a hot air oven in 1 hr at 100^0C to remove the volatile impurities. The glass substrates were mounted on a substrate holder with a heating arrangement and temperature was measured with the help of a fine wire chromel and alumel thermocouple. Molybdenum boat was used as a source

heater. The temperature of the substrate was maintained at 398 ± 5 K throughout the deposition. Constant rate of evaporation 3Å/sec was maintained throughout the sample preparation. Rotary drive was employed to maintain uniformity in film thickness. The substrate to source distance was optimized to be at 18.1 cm inside the vacuum chamber. The thickness of the film was measured by quartz crystal monitor.

3. Results and discussion

3.1Structural Studies

Raman spectroscopy was used to study the structure and composition of the film. Raman spectra of the films were recorded by using a Horiba's Lab Ram High Resolution spectrometer equipped with a multichannel detection system in the backscattering configuration. The incident laser light (λ=532 nm) could be focused on the sample within a spot of 1μ m in diameter.

Fig. 1 shows the Raman spectra of two different thicknesses of Cu_2S thin films. Raman studies of Cu_2S film indicated that peaks of 1000 Å and 7000 Å thickness are located at 472 cm^{-1} and 474 cm^{-1} respectively. It can be seen that the peak of 7000 Å thickness shifted to higher frequency from 472 to 474 cm^{-1} probably indicative of being a non-stoichiometric sulphur rich phase as reported earlier[9]. It is inferred that lower thickness film was Cu_2S and transferred to CuS at higher thickness.

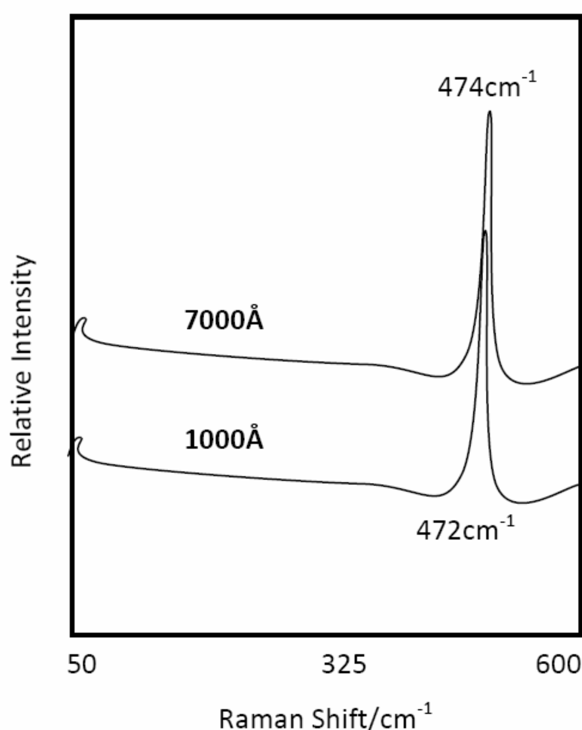

Fig. 1. Shows the Raman spectra of two different thicknesses of Cu_2S thin films.

3.2 Resistivity studies

The most commonly used technique for measuring resistivity is the four point probe method. The arrangement consists of PID controlled oven (model-PID-200 scientific equipment and services, Roorkee, India) in combination with low current source (model-LCS-01) and digital micro voltmeter. It consists of four collinear metal probes with sharpened tips, which are placed on the flattened surface of the material to be measured. Constant current is passed through the outer two probes and the potential difference is measured across the inner two probes. The nominal value of the probe spacing is equal to the distance of 2mm between the adjacent probes. The potential difference is measured using a high input impedance voltmeter.

Resistivity of thermally evaporated Cu_2S thin films were measured in the temperature range 303K- 453K from (20-100μA) for different thicknesses and is found between 10^{-8} to 10^{-6} ohm cm. The low resistivity of the films is due to the degenerate nature of the films. Fig. 2 shows variation of resistivity with inverse of absolute temperature for Cu_2S thin films of 1000 Å thickness at constant current. It is observed that resistivity decreases with increase in temperature and attains a minimum value called as critical temperature and further resistivity increases with temperature. The critical temperature is estimated within (383-403K). It may be inferred that film material behaves as semiconducting at lower temperature and metallic above critical temperature which is in good agreement with the earlier reports on Cu_2S thin films [10]. Moreover resistivity was found to increase with thickness upto 5600 Å and further decreases with increase in thickness for all the films analyzed (Fig. 3). In general it can be seen that resistivity is largely affected by grain size of the film. Since smaller the grain size the increased number of grain boundaries to be crossed by the carriers during electrical transport and hence results in increase in resistivity. Grain size (D) of Cu_xS film has been calculated using the Scherer's formula

$$D = \frac{k\lambda}{\beta \cos\theta} \quad (1)$$

where the constant K is the shape factor = 0.94, λ is the wavelength of x-rays (1.5406 for CuK_α), θ is the Bragg's angle and β is the FWHM and the values are given in table. It is found that there is gradual decrease in the grain size of the film with increasing film thickness. This is due to the growth of grains in the initial stage of film that show circular islands with lots of empty space between them. When the thickness of the film increases small grains grew up and coalescence of the grains occurred that results in decrease in grain size of the film [11]. However it is also observed that there is sudden increase in the grain size of the film at higher thickness [12]. Hence the decrease in resistivity beyond the critical thickness 5600 Å may be due to (i) the non- stoichiometric composition of the films at higher thickness (ii) increase in grain size of the film at

higher thickness. Therefore higher thickness film has strong influence on resistivity resulting in enhanced conductivity due to increase in grain size values.

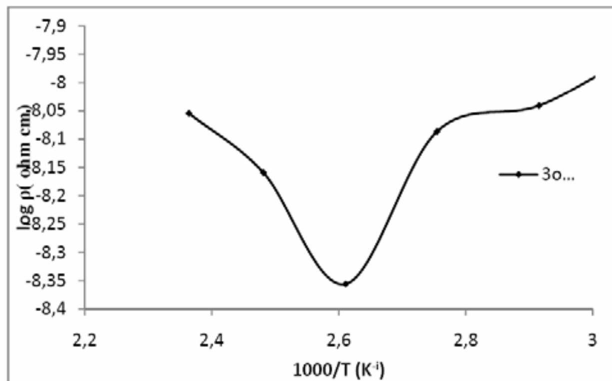

Fig. 2. Variation of resistivity with inverse of absolute temperature for Cu_2S thin films of 1000 Å thickness at constant current (I=30 µ A)

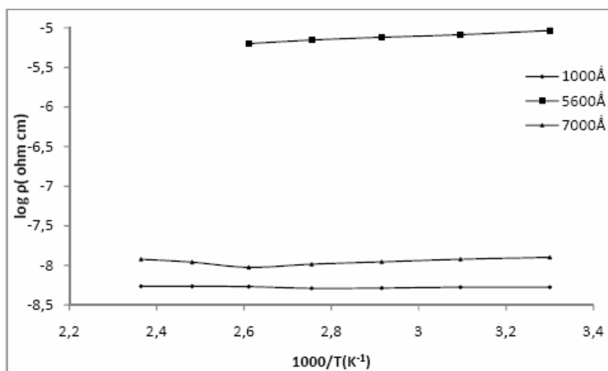

Fig. 3. Variation of resistivity with inverse of absolute temperature for Cu_2S thin films of different thicknesses at constant current (I=90µ A).

Band gap energy (E_0) of the material is determined from the slope of the line connecting the log ρ and 1/T and using the slope value in the following equation is

$$\rho = \rho_0 \exp (E_0/KT) \quad (2)$$

Where 'ρ' is resistivity at temperature T, 'ρ_0' is constant, 'K' is the Boltzmann constant and 'E_0' is the band gap energy. The calculated band gap are found to be 0.595 eV and 0.450 eV for Cu_2S thin film of 1000 Å and 7000 Å thickness respectively. The decrease in band gap energy with increase in film thickness is due to the presence of the internal defects in the film [13].

3.3 Optical studies

Optical properties of Cu_2S thin films were studied from the absorption spectra measured by a UV-Vis-NIR Spectrophotometer. The spectrophotometer has a wavelength range of 190 nm to 2500 nm with an accuracy of 0.3 nm. This spectrophotometer is interfaced with computer and the recorded spectrum is directly obtained from the computer.

Absorption coefficient measurements are essential for understanding the possible transitions of any semi-conducting material. From the absorption spectra optical band gap of the film for different thickness were calculated using the fundamental relation [14]

$$\alpha h \upsilon = A (h \upsilon - E_g)^n \quad (3)$$

Where 'hυ' is the photon energy, 'E_g ' is the band gap of the material 'A' and 'n' are constants 1e, n =2 for allowed direct transition and n= ½ for indirect transition. The optical gap value was determined from the absorption data by plotting $(\alpha h\upsilon)^n$ as a function of hυ (Tauc's plot), through extrapolation of linear portion of the plot that intercept on hυ axis. Fig. 4 shows the plot of absorption coefficient versus incident photon for direct band gap of Cu_2S films of two different thicknesses. Energy dependence of the optical absorption coefficient exhibit two distinct regions, a high energy threshold and a low energy threshold region corresponding to two absorption mechanisms [15]. The measured direct transitions are found to lie in the range (1.9 to 1.2 eV) that agrees with the value reported earlier for Cu_2S thin films [16]. The direct band gap of Cu_2S thin films is found to be thickness in- dependent and this decrease in band gap with increase in film thickness is due to large density of dislocations [17]. The indirect transitions are associated with changes in the lattice structure and stoichiometry. The coefficient of absorption (α) is related to coefficient of extinction (k) by

$$\alpha = \frac{4\pi k}{\lambda} \quad (4)$$

where $'\lambda'$ is the wavelength of the incident radiation[18]. The extinction coefficient (k) can thus be calculated from the above relation

$$k= \frac{2.303\, \lambda \log (1/T_0)}{4\pi d} \quad (5)$$

where 'T_o' is the transmittance and 'd' is the thickness of the film. From the plot of extinction coefficient versus photon energy curve (Fig. 5) it is observed that extinction coefficient decreases with increase in photon energy and then increases with further rise in photon energy at lower thickness [19]. Moreover extinction coefficient is found to decrease at higher thickness which may be due to deviation in the stoichiometry of the film at higher thickness. The refractive index of the film (n) is given by

$$n= \frac{1}{2t\Delta(\frac{1}{\lambda})} \quad (6)$$

where 't' is the thickness of the film. Refractive index has been calculated for various thickness of Cu_2S thin film using (6) and the values are reported in table. From the table it is inferred that refractive index increases with film

thickness. Further refractive index decreases with increase in photon energy (Fig. 6). It is observed from the graph that the film shows sharp decrease in the refractive index variation from 2.2 to 1 in the range 1.2 to 1.9 e V and gradual decrease in the refractive index beyond 1.9e V [20].

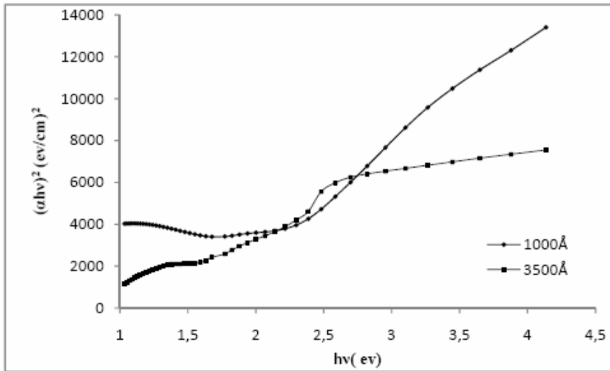

Fig. 4. Plot of absorption coefficient versus incident photon for direct band gap of Cu_2S films of two different Thicknesses.

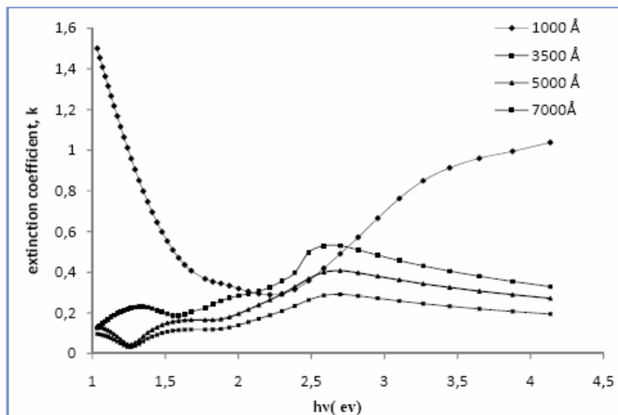

Fig. 5. Plot of extinction co-efficient versus photon energy for Cu_2S thin films

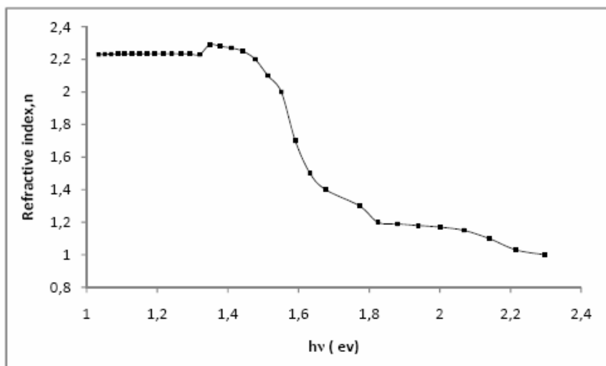

Fig. 6. Variation of refractive index with photon energy for Cu_2S thin films

Optical conductivity (σ_o) of the film is given by the relation

$$\sigma_o = \frac{\alpha n c}{4\pi} \tag{7}$$

where 'α' is the absorption coefficient, 'n' is the refractive index of the film and 'c' is the velocity of light [21]. Fig. 7 shows the variation of optical conductivity with photon energy for different film thickness. It is observed from the figure that the optical conductivity increases with photon energy and this increase in optical conductivity is due to high absorbance of the film at higher energy level [19]. Moreover the optical conductivity is found to decrease with increase in film thickness.

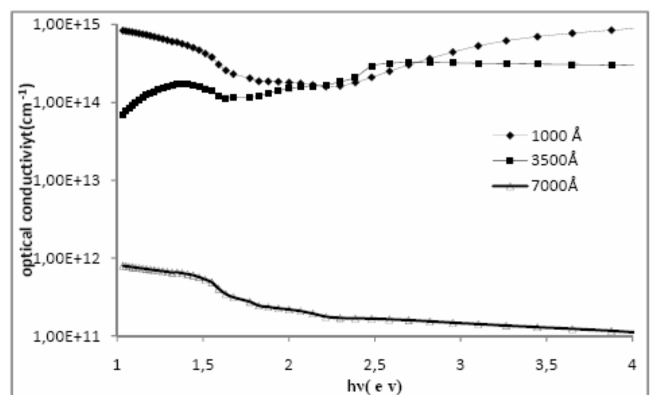

Fig. 7. Variation of optical conductivity with photon energy for Cu_2S thin films of various thicknesses

3.4 Thermo EMF studies

A simple method, which is widely used to determine the conductivity type of a specimen, is hot probe method. Two fine metal probes preferably made of stainless steel or nickel is placed on the semiconductor sample and a zero centered galvanometer is connected between them. One of the probes is kept at room temperature and the other is heated to about 800^0C. It is convenient to use a miniature soldering iron tip as the hot probe. The hot probe heats the semiconductor beneath it so that the kinetic energy of free carriers in this region is increased. Therefore the carriers diffuse out of the hot region at a faster rate rather than they diffuse into this region from the adjacent low temperature regions. The polarity of the hot probe indicates whether the semiconductor is n or p-type. From the hot probe method it is observed that the current flows from to the hot probe cold probe for all the film studied in the present work and is inferred that, Cu_2S film exhibits p-type conductivity.

3.5 Hall Effect Measurement

Hall effect measurement was carried out in an effort to study the carrier type of the film. Hall measurements were carried using Van der Pauw method [22]. All

measurement was carried out at room temperature on glass plate. These glass plates were pressed against a second plate with four contacts contacting thin film at four corners. The magnetic flux density in the Hall effect measurement was 1.88 tesla and the resulting hall voltage had an order of magnitude 50µV.

Carrier mobility (μ_h) for the film is calculated by using the following equation

$$\mu_h = \frac{\sigma}{R_H} \quad (8)$$

Where ' R_H' is the Hall coefficient and 'σ' is the conductivity of the material. The value of carrier mobility slightly increases from 3 to 6 $cm^2\ V^{-1}\ sec^{-1}$, the higher values corresponds to the stoichiometric composition of Cu_2S thin films [23]. The decrease in value of carrier mobility at higher thickness is due to the decreasing copper content of the film ie, decreasing in the value of x in Cu_xS thin films. It is observed from Fig. 8, that carrier mobility of the film raises linearly upto thickness 5000Å and once the copper content of the film begin to decrease, the carrier mobility of the film decreases. Hall coefficient (R_H) of the film can be calculated by using the relation

$$R_H = \frac{t\,V_H}{IB} \quad (9)$$

where 'V_H' is Hall voltage,'t' is the film thickness, 'B' is magnetic induction, 'I' is the magnetic flux intensity. From the measured Hall coefficient, carrier concentration (n) of the film can be calculated by using the relation

$$n = eR_H \quad (10)$$

where 'e' is the charge of the electron and the values are reported in the table. Carrier concentration of the film is found to be thickness dependent (Fig. 9). Compared with lower thickness, higher thickness Cu_2S thin films has much higher carrier concentration around $10^{22}\ cm^{-3}$, which results in decrease in resistivity of the film [24, 25]. The increase in carrier concentration of the film is due to the improvement in the crystallinity of the film. Higher thickness film has lower mobility value and this is mainly due to higher carrier concentration. Thus carrier concentration corresponds to copper vacancies of V_{Cu} in Cu_xS thin films. The mean free path (l) is calculated by using the following relation

$$l = \frac{h(3n)^{\left(\frac{1}{3}\right)}}{2e\pi^{\left(\frac{1}{3}\right)}}\mu \quad (11)$$

where 'e' is the charge of the electron, 'h' is Planck's constant, 'n' is the carrier concentration and 'µ' is the carrier mobility and the values are reported in table. It is observed from the table that mean free path of the film increases with film thickness.

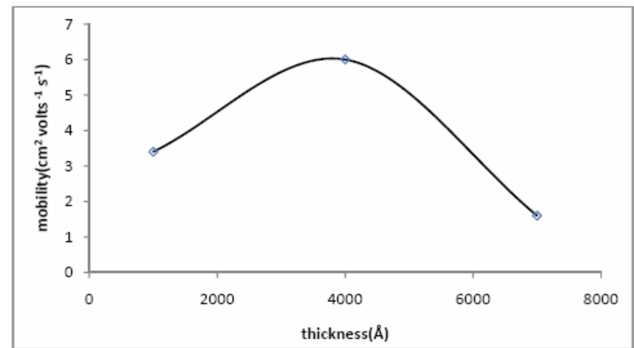

Fig. 8. Variation of mobility with film thickness for Cu_2S thin films

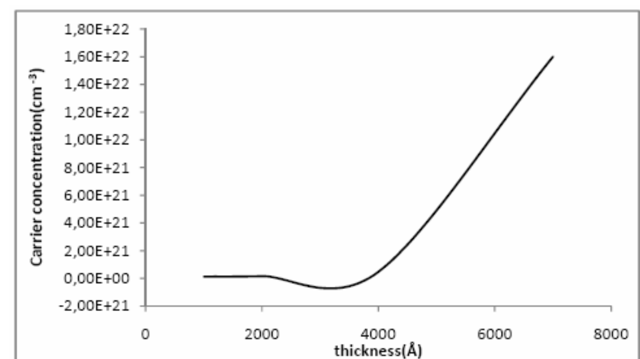

Fig. 9. Variation of carrier concentration with film thickness for Cu_2S thin films

3.6 Electrical Studies

Current- voltage characteristics of the Cu_2S thin films were studied by employing digital micro ammeter in series with the capacitor and the voltage source. All the studies were performed under the vacuum of about 680 mm Hg. Current voltage behavior was studied in the temperature range 300-400K and the temperature during measurements was maintained using variable voltage transformer. A copper constantan thermocouple is used for the temperature measurements and potential of 20 volts was applied using DC regulated power supply in series with the digital voltmeter.

Fig. 10 shows current versus voltage characteristics of evaporated Cu_2S thin films of two different thicknesses at constant current measured at room temperatures. It is seen that the curve exhibit ohmic type of conduction in the lower fields, indicating that the current controlled by thermally generated carriers [26, 27] and non-ohmic in the higher fields respectively. Electrical conductivity (σ_e) of the film is calculated using the relation

$$\sigma_e = \frac{2\pi\sigma_o}{\alpha} \quad (12)$$

where' σ_o' is the optical conductivity and 'α' is the absorption coefficient of the film. It is observed that

electrical conductivity increases with increase in film thickness [21].

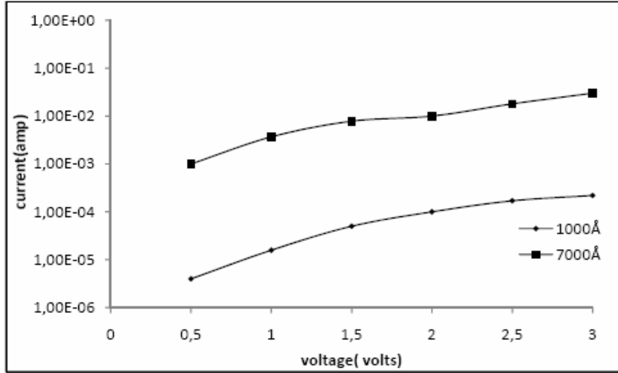

Fig. 10. Log current versus log voltage for Cu_2S thin films of two different thicknesses at room temperature

Photosensitivity of the semiconductor film can be expressed as

$$S= \frac{I_{light}-I_{dark}}{I_{dark}} \tag{13}$$

where I_{light} and I_{dark} are the currents measured under illumination and in dark respectively. Fig. 11 shows the photo response characteristics of as grown Cu_2S thin films of 1000 Å thickness. The graph show that photo sensitivity increases with increase in light intensity. Moreover highest photo sensitivity of Cu_2S thin films has been observed at 800 W/ cm ^{2} illumination for 1000 Å thickness.

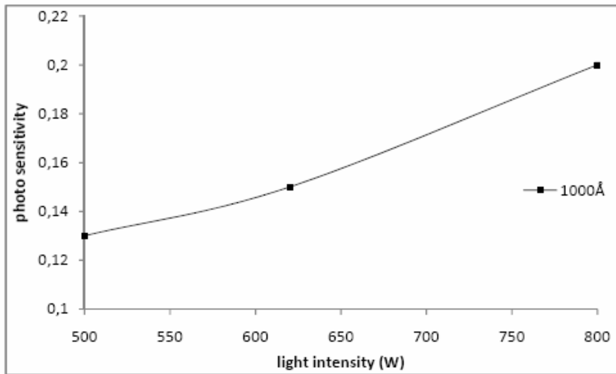

Fig. 11. Variation of photosensitivity with light intensity for Cu_2S thin films of 1000 Å thickness at 10 V.

3.7 Di-electric Studies

The complex dielectric constant is fundamental intrinsic material property. The real part of it is associated with the term that how much it will slow down the speed of light in the material and imaginary part gives that how a dielectric absorb energy from electric field due to dipole motion. The real 'ε_r' and imaginary parts 'ε_i' of the dielectric constant were determined using the relation [28],

$$\varepsilon_r = n^2 - k^2 \tag{14}$$

and

$$\varepsilon_i = 2nk \tag{15}$$

where 'n' is the refractive index and 'k' is the extinction coefficient of the film. Therefore,

$$\varepsilon = \varepsilon_r + \varepsilon_i = (n+ik)^2 \tag{16}$$

Fig. 12 shows the variation of dielectric constant with photon energy for Cu_2S thin films. It is observed from the figure that both real and imaginary part of dielectric constant decrease with increase in photon energy and this decrease in dielectric may be due to the absorbance associated with free charge carriers [19].

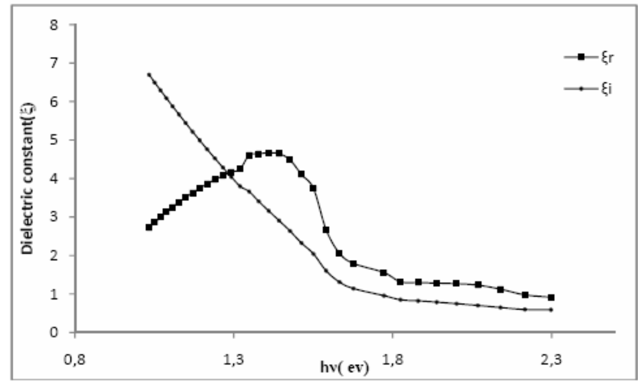

Fig. 12. Variation of real and imaginary part of dielectric constant with photon energy for Cu_2S thin films

Dissipation factor (tan δ) is a measure of loss rate of power in a dissipative system ie., electric power is lost in all dielectric material in the form of heat. Dissipation factor can be calculated by using the following equation

$$\text{Tan } \delta = \frac{\varepsilon_i}{\varepsilon_r} \tag{17}$$

Fig. 13 shows the variation of dissipation factor with photon energy for Cu_2S thin films. It is evident from the graph that dissipation factor decreases with increasing value of photon energy ie, electric loss in the form of heat in the Cu_2S thin film is minimized with increasing photon energy.

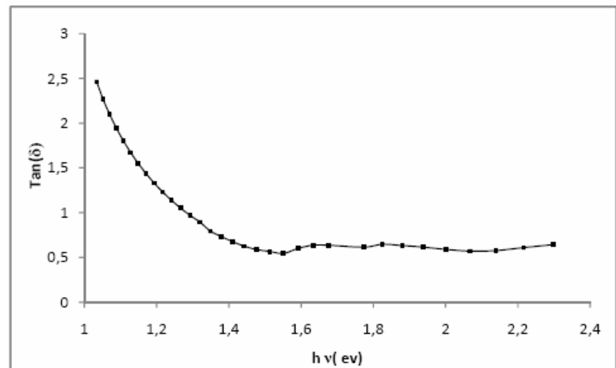

Fig. 13. Variation of dissipation factor with photon energy for Cu_2S thin films.

4. Conclusion

Cu_2S thin films with good crystallinity have been deposited on glass substrates by vacuum evaporation method. Cu_2S thin films of higher thickness has relatively high carrier concentration around 10^{22} / cm^3, and slightly much lower Hall mobility of about 1.6 cm^2 /VS compared with the semiconducting Cu_2S film of lower thickness. The activation energy and optical band gap of Cu_2S thin films were found to be thickness dependent. The measurement of thermo-emf confirms p-type conduction mechanism of Cu_2S. The refractive index, extinction coefficient, optical conductivity and the dielectric properties of Cu_2S films were also studied. The values of the band gap energy obtained for the Cu_2S thin film are in good agreement with the literature data.

Table. Carrier concentration, carrier mobility, Hall coefficient, electrical conductivity, mean free path, grain size and optical band gap of Cu_2S thin films of different thickness.

Thickness (Å)	Carrier concentration (n)(cm^{-3})	Hall mobility (μ)(cm^2/VS)	Hall Co-efficient (R_H)(cm^3/C)	Electrical conductivity (σ_e)(Ω^{-1} cm^{-1})	Refractive index(n)	Activation energy (eV)	Mean free path (l)(Å)	Grain size (nm)	Optical band gap (ev)
1000	1.0* 10^{19}	3.4	0.270	1	1.08	0.595	151	207	1.9
5000	1.5 * 10^{19}	6	0.180	4.7	2.63	0.500	306	19.77	1.4
7000	1.6* 10^{22}	1.6	0.0009	7	2.7	0.450	836	103	1.2

References

[1] Miao Chen, Jing Zhao , Xiaocui Zhao, Electrochimica Acta **56**, 5016 (2011).
[2] Carolyn G. Munce, Gretel K. Parker, Stephen A. Holt, Gregory A. Hope, Colloids and Surfaces A: Physicochem. Eng. Aspects **295**, 152 (2007).
[3] S. D. Sartale, C.D. Lokhande , Materials Chemistry and Physics **65**, 63 (2000)
[4] Nourhene Kamoun Allouche, Tarak Ben Nasr, Cathy Guasch, Najoua Kamoun Turki, C. R. Chimie **13**, 1364 (2010).
[5] I. Grozdanov, M. Najdoski, J. Solid State Chem. **114**, 469 (1995).
[6] K. Malle, Bolga, V. Tiit, M. Vaidek, Thin Solid Films **38**, 125 (1999)
[7] S. R. Das, V. D. Vankar, P. Nath, K. L. Chopra, Thin Solid Films **51**, 257 (1978).
[8] M. Ramya, S. Ganesan, Iranian Journal of Materials Science & Engineering, **8**, 2 (2011).
[9] Sheng-Yue Wang,Wei Wang, Zu-Hong Lu, Materials Science & Engineering **B102**, 184 (2003).
[10] H.M. Pathan, J.D. Desai, C.D. Lokhande, Appl. Surf. Sci. **202**, 47 (2002).
[11] S. Lalitha, R. Sathyamoorthy, S. Senthilarasu, A. Subbarayan, K, Natarajan, Solar Energy Materials and Solar Cells **82**, 87 (2004).
[12] A. Loptez Otero, Journal of Crystal Growth **42**, 157 (1977).
[13] A.U. Ubale, D.M. Choudhari, J.S. Kantale, V. N. Mitkari, M.S. Nikam, W.J. Gawande, P.P. Patil, Journal of Alloys and Compounds **509**, 9249 (2011).
[14] S.S. Shinde, P.S. Shinde, C.H. Bhosale, K.Y. Rajpure, Solid State Sci.**10**(9), 1209 (2008).
[15] R.Sathyamoorthy, Sa.K.Narayandass, D.Mangalraj, Solar Energy Materials and Solar Cells **76**, 339 (2002).
[16] S. Senthilarasu, R. Sathyamoorthy, S. Lalitha, A. Subbarayan, K.Natarajan, Solar Energy Materials and Solar Cells **82**, 179 (2002).
[17] A.C.Rastogi, S.Salkalachen Thin Solid Films **97**, 191 (1982).
[18] N. Suzuki, K. Sawai, S. Adachi, Journal of Applied Physics, **77,** 3 (1995).
[19] S. U. Offiah, P.E. Ugwoke, A.B.C. Ekwealor, S. C. Ezugwu, R.U. Osuji, F. I. Ezema, Digest Journal of Nanomaterials and Biostructures **7**, 165 (2012).
[20] P. A. Ilenikhena, African Physical Review **2**, 0007 (2008)
[21] J. I. Pankove, "Optical Processes in Semiconductors" Dover Publications, Inc. New York, p-91(1971)
[22] Van der Pauw L. J., Philips' Technische Rundschau **20**, 230 (19.58/59).
[23] R. Wagner, H.D. Wiemhofer, Journal of physics and chemistry of solids **44**, 801 (1983).
[24] Y.B. He, A. Polity, I. O. sterreicher, D. Pfisterer, R. Gregor, B.K. Meyer, M. Hardt, Physica **B 308–310,** 1069 (2001).

[25] P. Parreira, G. Lavareda, A. Amaral, A.M. Botelho do Rego, O. Conde, J. Valente, F. Nunes, C. Nunes de Carvalho, Journal of Alloys and Compounds **509**, 5099 (2011).
[26] N. Mazumdar, R. Sarma, B. K. Sarma, H. L. Das, Bull. Mater.Sci, **29**(1) 11 (2006).
[27] M. Ramya, S.Ganesan, Optoelectron. Adv. Mater. – Rapid Comm. **5**(9), 936 (2011).
[28] E. Marquez, A. M. Bernal-Oliva, J. M. Gonzalez-Leal, R. Prieto-Alcon, A. Ledesma, R. Jimenez-Garay, I. Martil, Mater. Chem. and Phys**.** **60,** 231 (1999).

*Corresponding author: ramsthangam@gmail.com